JOURNAL OF SOLID STATE CHEMISTRY 104, 149–159 (1993)

Adsorption of Gold and Silver on the Tungsten (110) Surface Studied by Field Emission Microscopy

J. P. JONES

School of Electronic Engineering Science, University of Wales, Bangor, United Kingdom

Received October 29, 1992; accepted November 9, 1992

The field emission characteristics of the tungsten (110) surface before and after diffusive invasion by vapor deposited gold and silver have been investigated using probe-hole microscopy. Adatoms adsorbed on the terraces which surround W(110) extend the plane area producing an apparent increase in work function before invasion takes place. At temperatures above 500 K, the terraced regions are rearranged by adsorbed gold but not by silver. Once populated the plane is rapidly covered with a complete monolayer of the metal, and invasion by gold is consistent with a mechanism of nucleation and 2-dimensional growth. Both the work functions of the monolayers and the coverages at which they form are in substantial agreement with findings on macroscopic W(110) using LEED and related techniques.

1. Introduction

Field ion microscopy shows that the 110 plane on a thermally annealed tungsten tip offers a relatively large area with a high degree of structural perfection (*1*). This, together with the experimental (*2*) and theoretical (*3*) evidence that in field emission the 110 plane behaves as a free electron metal, makes it an attractive substrate on which to study adatom behavior and epitaxy. When adsorption of gold on tungsten (110) was examined, (*4*, *5*), it was particularly notable that the adsorbate atoms are weakly bound on the (110) surface, readily departing by surface diffusion into the surrounding regions, to sites which presumably have higher binding energy. When the gold adatom population in the region surrounding the clean plane becomes sufficiently high, inundation of the plane rapidly establishes a permanent population of adsorbate atoms. Similar behavior has been seen in other systems (*6*, *7*). However, unlike other invasion processes, gold diffusion onto W(110) is invariably preceded by a small increase in the work function $\Phi(110)$ of the plane, and inundation does not lead to the immediate establishment of a coverage-independent work function. It was suggested (*5*) that the observed increase in work function might be due, not to the presence of gold on the plane, but to an effective increase in the extent of the plane area produced by the presence of surrounding gold, because this would reduce the local applied field F_{loc} which, in the Fowler–Nordheim (FN) analysis, is indistinguishable from an increase in the work function. In an attempt to clarify the invasion process and the conditions that precede it, we have examined the invasion of W(110) by gold and silver, and sought to distinguish change in $\Phi(110)$ from change in F_{loc} and the effective emitting area A.

0022-4596/93 $5.00

2. Measurement of Surface Properties

2.1. Work Function Φ and Local Field Strength F_{loc}

The FN model including the electrostatic image term yields a curve of slope S(FN), where

$$S(\mathrm{FN}) = \frac{d\log(i/V^2)}{d(10^4/V)} = -2.97 \times 10^3 \times \frac{\phi^{3/2}}{\beta} \times s(y), \quad (1)$$

where i is the current (A). $s(y)$ is an elliptic function having a value close to unity. The applied field F (volts/cm) is averaged over the emitting area in question, and is related to the applied voltage V through the field enhancement factor β:

$$F = \beta V. \quad (2)$$

Equation (1) is commonly used to derive changes $\Delta\Phi$ in Φ since, if the emitting surface changes from state 1 to state 2, the change in work function is given by

$$\Delta\Phi = \Phi_1 \left[\frac{S_2(\mathrm{FN})^{2/3}}{S_1(\mathrm{FN})^{2/3}} - 1\right]. \quad (3)$$

Work functions of emitting areas selected by the probe hole have been measured by assuming a value for the average work function of the total emitting area, measuring S(FN) for both the total area and the probed areas, and applying Eq. (3) so that

$$\Phi(\text{probed area}) = \Phi(\text{total area}) + \Delta\Phi. \quad (4)$$

Application of equation 3 assumes that F and the elliptic function $s(y)$ do not alter between the two states. $s(y)$ varies very little under the prevailing experimental conditions (*8*), and this is also generally true of F when the measured changes refer to the same examined areas. However, when the probe hole technique is used, the local field at the probed region cannot be assumed to be the same as the average field F acting on the emitting tip. This is particularly true for the (110) tungsten surface, which, on a thermally cleaned tip, is an extensive plane at the center of which the field F(110) is believed to be significantly less than F, due to the larger local radius of curvature (*9*). Following Ehrlich and Plummer (*2*), we therefore assume that the true work function of (110) is 5.25 eV, and that for the clean plane the value of β can be obtained from S(FN) using Eq. (1). The effect of the image potential has not been included because it is small and does not substantially affect the interpretation of our findings. Possible patch field effects have been shown to be unimportant in the prevailing circumstances (*9*), and are therefore omitted.

2.2. Local Current Density J_p and Emitting Area A

van Oostrom (*8*) has shown that the current density J, and the emitting area A are readily derived from FN data since $S(\mathrm{FN})/V$ is a linear function of log J and is only weakly dependent on Φ. By choosing an i_p–V_p pair, K can be obtained from $K = S(\mathrm{FN})/V$ and the current density in the probed area, J_p, from tabulated values of K (*8*). A is then calculated from $A = i_p/J_p$. Areas obtained in this way from the present data are estimated to be accurate to within 5%.

3. Experimental Procedure

The probe-hole field emission microscope has been described previously (*10*). Tungsten tips, formed by electropolishing short lengths of 0.005-in. diameter outgassed wire, were spotwelded to hairpin loops of the same wire and provided with short potential leads for measurement and control of the tip temperature. Temperatures, measured from the resistance of the central portion of each loop, were controlled by a servocircuit to within ±2 K, and are accurate

to within ±5 K over the range employed, 300–800 K. The applied imaging voltage, accurate to within 0.05%, was derived from a precision high voltage source (Fluke Model 408B). The total emitted current, which was in the range 1–100 nA, was measured using a Keithley Model 602 amplifier, while the much smaller probe hole currents of 0.001–10 pA were measured with a Keithley Model 616 digital amplifier. The tip image was steered magnetically using a small rotatable dc electromagnet and the (110) center was located by adjusting the image to give the minimum current through the probe hole. The total energy distribution of the electrons emitted by the probed region was obtained using the retarding-field method, by simultaneously recording i_p and a smoothly varying bias voltage V_b applied between tip and collector (*11*). Work functions computed from i–V data by standard Fowler–Nordheim analysis were subjected to a point-throwing routine which held the errors (computed by least squares analysis) below 0.02 eV. Gold was condensed onto the tip from a bead of metal (Johnson Matthey, Specpure) enclosed in an electrically heated spiral of outgassed 0.005-in. diameter tungsten wire, sited 2 cm from the tip so as to deliver gold vapor to the side of the tip and not directly to the visible 110 plane. Reproducible gold doses were delivered by precisely controlling and timing the source current. Earlier work (*12*) had established that the average work function of the emitting tip attains a maximum value at an adatom population of $6.7 \pm 2 \times 10^{18}$ gold atoms per m^2. This was used to calibrate the gold flux. The assembled microscope was vacuum-processed to attain a pressure below 1×10^{-9} Pa, the glass envelope sealed, and the system gettered using molybdenum to reduce the pressure of active gases to below 1×10^{-11} Pa as judged by the rate of contamination of the cleaned tip surface. Frequent ion pumping was necessary to maintain the partial pressure of helium below 1×10^{-9} Pa. Examination of the 110 plane requires that relatively high emission currents ($\sim 1 \times 10^{-6}$ A) be drawn for periods of 10–15 min, during which time gas evolution from the phosphor screen can be a significant source of contamination. The screen was therefore outgassed by imaging at 3×10^{-6} A for periods totalling 30 min and, after gettering, the surface could be imaged for periods of 20 min at the maximum working current, (5×10^{-7} A), without incurring significant contamination.

4. Experimental Results

4.1. Gold

Processes which occur on the imaged surface can be conveniently followed by monitoring the change ΔV_i in V_i, the voltage which must be applied to draw a selected field emission current i. This permits changes in surface conditions to be monitored efficiently, and these changes can be related to physically meaningful properties, such as the change in work function or emitting area, by acquiring the necessary data in separate experiments. We have adopted this strategy, and Fig. 1 shows ΔV_t for the total emission current $i_t = 5 \times 10^{-7}$ A and ΔV_p for the probe hole current $i_p = 1 \times 10^{-12}$ A. The tungsten surface was prepared by thermally cleaning the tip at 2500 K for 10 sec and annealing at 1500 K for 20 sec. Each dose of gold was condensed on the tip surface at 78 K in zero field, spread by diffusion at a chosen temperature for a defined time, usually 30 sec; V_t and V_p were then measured at 78 K. Experiment showed that 30 sec was generally sufficient to effectively complete all change, yielding a quasi-equilibrium state.

The maximum in the ΔV_t vs gold dose corresponds to a gold adatom density of $6.7 \pm 2.0 \times 10^{18}$ atoms/m^2, (*12*) and establishes the mean surface adatom population as successive doses of gold are added. The characteristic sharp decrease in ΔV_p of (110)

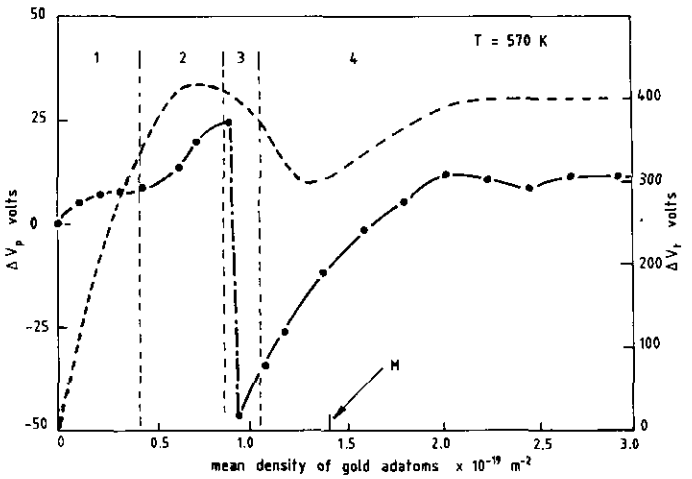

FIG. 1. Effect of adsorbed gold on emission from the total tip ΔV_t, (---), and from the 110 plane, ΔV_p. Successive doses of gold are condensed onto a tungsten surface at 78 K and heated for 30 sec at the indicated temperature. *M* corresponds to the density of atoms in the 111 plane of gold. Regions 1 to 4 are considered separately in the text.

depicted in Fig. 1 is thought to mark the invasion of the plane by gold diffusion from its surroundings, and Fig. 2 shows that the coverage at which this occurs decreases as the spreading temperature is increased. Figure 3 presents a ΔV_p-coverage characteristic taken at a temperature which yields the largest increase in ΔV_p together with the results of FN data taken at the arrowed points, to yield $\Phi(110)$, A, and β at the center of the plane. The behavior of ΔV_p can be conveniently divided into four regions as indicated on Fig. 1:

(1) the small, reproducible, and temperature-independent increase in ΔV_p

(2) a further rise in ΔV_p which increases as the spreading temperature is raised

(3) the sharp drop which is thought to mark the invasion of the plane

(4) the establishment and consolidation of a gold overlayer.

Region 1. Gold on the 110 plane reduces $\Phi(110)$ (*5*); thus any increase in work function cannot be due simply to gold on the plane. The initial increase in ΔV_p is accompanied by a 0.1 eV increase in $\Phi(110)$ and a reduction in the emitting area A. Identical thermal treatment of a clean tungsten surface produces no change, indicating that the observed changes are not due to impurity in the tungsten.

Figure 4a presents a typical field ion micrograph of a thermally cleaned tungsten surface, and shows that the diameter of the 110 plane approaches 30% of the tip radius (see below). On this basis the central plane on the tip under examination is 24 nm in diameter; thus a probe sited at the plane center examining an emitting area approximately 4 nm in diameter should not receive any contribution from the surrounding terraced regions. However, changes in these relatively remote surroundings can alter the field at the plane center by altering β.

Adsorption of gold atoms is most likely to take place at the step edges (Fig. 4b), increasing the radius of the plane and reducing the local field strength. An attempt was made to measure β independently by examining the energy distribution using the technique developed by Young and Clark (*11*),

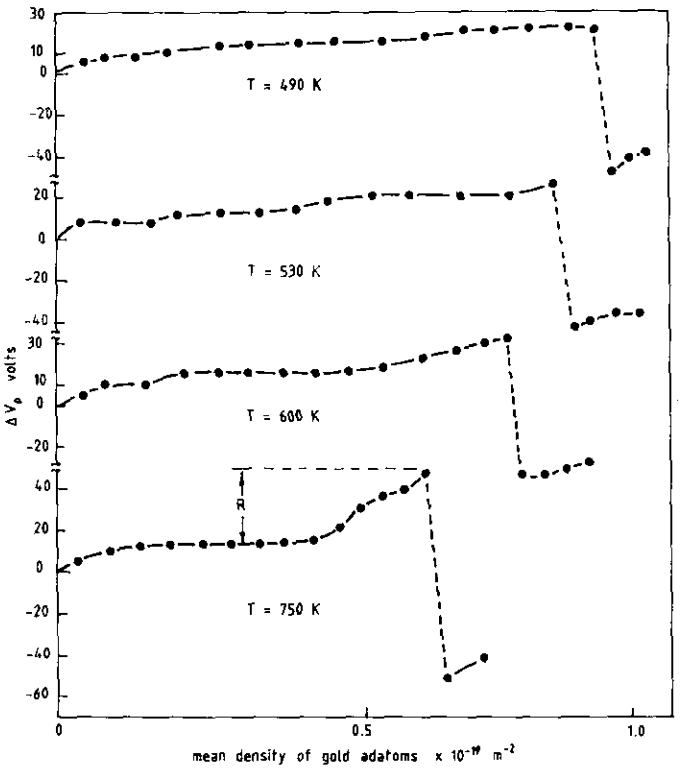

FIG. 2. Change in the invasion characteristic with spreading temperature T, showing the decrease in the adatom density at invasion and the increase in the rise R with increasing temperature. Alternate experimental points have been omitted for clarity.

but the result was inconclusive because the total error in the measurement was comparable with the observed change. The emission profile of the plane, obtained by magnetically scanning the probe hole across the plane (*9*), showed no detectable broadening on adsorption of relevant amounts of gold.

If we attribute all the measured change in Φ(FN) to alteration in F(110), then it follows from Eq. (1) that the latter must decrease by a factor of 0.975, and β must therefore decrease by the same amount. Measurement shows that the diameter of the first terrace ring, Fig. 4a, is greater than that of the central plane by a factor of approximately 1.11. Assuming this to apply to the examined surface, gold adsorbed on the first terrace will increase the radius of the central plane by 11%. Figure 4b shows a section of the terrace structure in which the indicated tip dimensions were derived by equating the diagonal distance between two {211} planes with the tip radius, and calculating the latter from the FN data.

There is a parabolic decrease in F(110) from the plane edge to its center (*9*). Based on this, and assuming that the field at the plane edge is unchanged by expansion, it can be shown that an increase in radius by 11% will reduce the field at the center, reducing β by a factor of 0.925, which yields an apparent increase in Φ(110) of 0.3 eV. This is probably an overestimate because the field at the plane edge is likely to increase

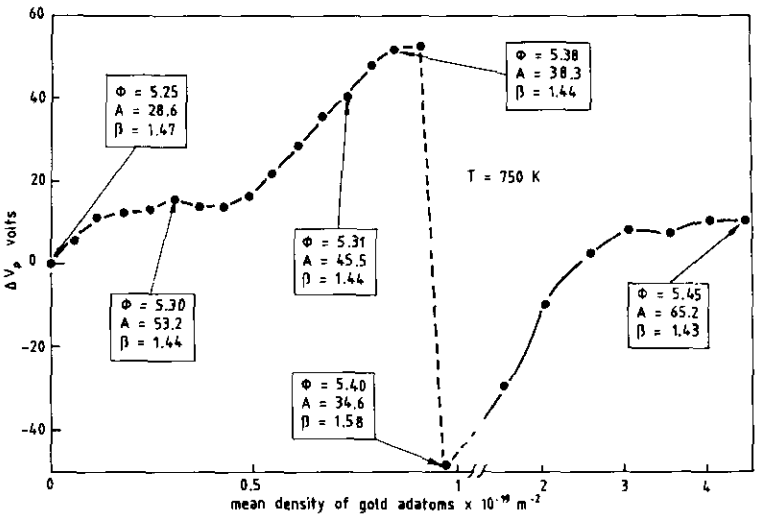

FIG. 3. Adsorption characteristic of gold on W(110) for $T = 750$ K which yields the maximum rise R, showing the work function ϕ (eV), the emitting area A (nm^2), and the field enhancement factor $\beta \times 10^{-4}$ at the indicated points.

slightly. Figure 3 shows that β decreases by a factor of 0.98, in agreement with the above model. Thus, bearing in mind the uncertainty in the true dimensions of central plane and terraces on the surface under examination, we conclude that plane expansion can certainly account for the observed increase in $\Phi(110)$.

Adsorption of gold on the surroundings reduces A to about half its original value. Reduction of A has been observed for adsorbates such as nitrogen (*8*), and attributed to modification of the tunnelling barrier by the adatom, but with no adsorbate present in the examined area, change in A cannot be attributed to this cause. It seems possible that the reduction in local field through plane expansion will be accompanied by a change in the shape of the 3-dimensional tunnelling barrier, but this will not appear in the Fowler–Nordheim model which treats the barrier as 1-dimensional.

Region 2. Despite the considerable increase in ΔV_p there is no significant change in Φ or β, but there is a small decrease in A. The fact that the rise in ΔV_p is dependent on the treatment temperature T, Fig. 2, suggests that it results from a process of surface diffusion. Field ion microscopy has shown that in the presence of gold the environs of (110) can be rearranged at temperatures as low as 400 K to form a tungsten surface with improved structural perfection, of the plane edges (*13*). In Fig. 2, every dose of gold was heated to the stated temperature for 30 sec, and since each dose was identical, differences between the degree of change produced in 30 sec at different temperatures will crudely reflect differences in the rates of the process observed.

The total change in ΔV_p (R in Fig. 2), divided by N, the relevant number of heating periods, is then a measure of the rate of change. Figure 5 shows an Arrhenius plot of $\ln(R/N)$ vs $1/T$ which yields an activation energy of 0.4 ± 0.1 eV for this process. This is comparable with the value 0.48 ± 0.04 eV observed for diffusion of sub-monolayer gold over the environs of (110) (*14*). Thus it seems probable that although at the highest

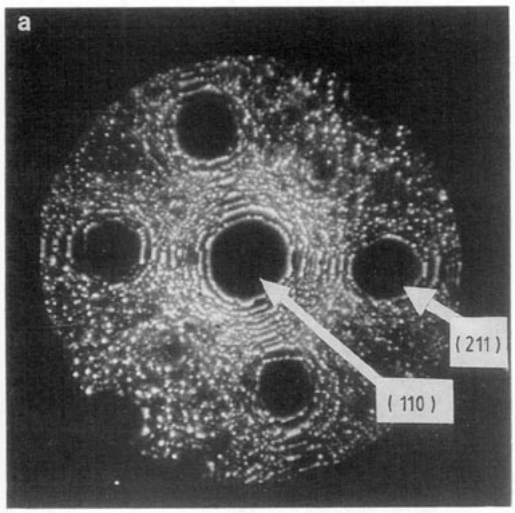

FIG. 4. (a) Field ion image of thermally clean and annealed tungsten showing the large central 110 plane, its surrounding terraces, and four {211} planes. (b) Schematic section through the plane and first terrace, having the approximate dimensions of the probed surfaces, illustrating plane expansion by adsorbed gold.

and none of the features seen in regions 1 and 2 are observed.

Region 3. The sharp fall in ΔV_p clearly marks the invasion of the central plane by gold and is seen with both the head-on and side-on sources.

The process of plane invasion has been analyzed elsewhere (*6*), showing that the ratio of the adatom density on the plane, n_p, to that on the surroundings, n_s, depends on temperature T and is given by

$$\frac{n_p}{n_s} = \exp\left[\frac{H_p - H_s}{kT}\right], \qquad (5)$$

where H_p is the binding energy of a gold atom on the 110 plane, and that on the surroundings, H_s, is dependent on adatom density according to

$$H_s = H_s(0) - a \cdot n_s, \qquad (6)$$

where $H_s(0)$ is the binding energy at zero coverage. As the population of adatoms on the surroundings rises their binding energy falls until, at a critical coverage, the central plane population rises to the point when a

temperatures other factors are limiting the observed change (Fig. 5), surface diffusion is responsible for much of the rise R in Fig. 2.

Region 2 is therefore believed to result from diffusion of gold and tungsten atoms in association, leading to improved structural perfection of the plane edges. This has a small effect on the emitting area A, while Φ and β remain unaltered (Fig. 3), presumably because the size of the central plane and the surrounding terrace structure do no change substantially during this process. The effects seen in regions 1 and 2 are in marked contrast to the behavior observed when gold is deposited directly on (110) from a head-on source and heated at comparable temperatures (*5*). In this case gold is lost from the terraces by diffusion down the tip shank,

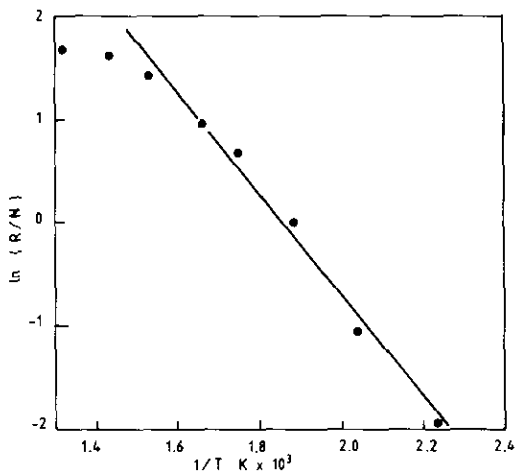

FIG. 5. Arrhenius plot of $\ln(R/N)$ vs $1/T$, where R is the rise in indicated on Fig. 2, N is the number of doses of gold over which R is achieved, and T is the spreading temperature.

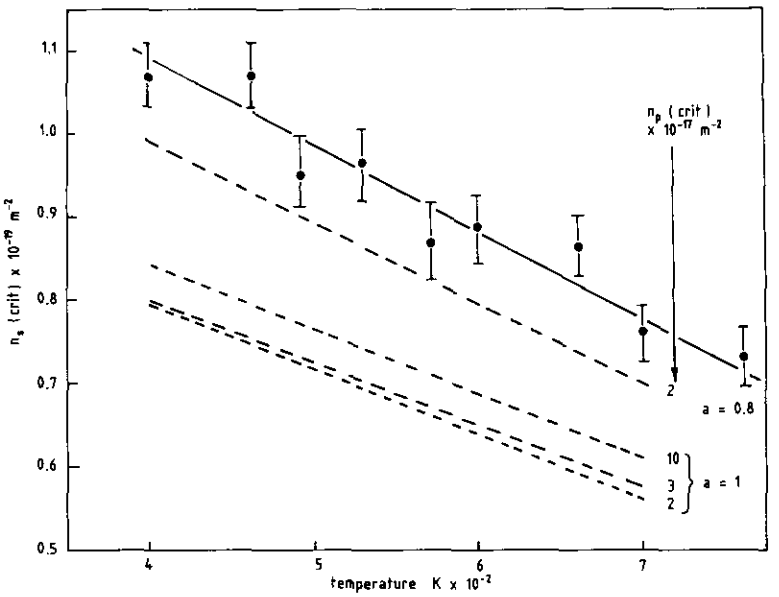

FIG. 6. Invasion of W(110) by gold. Plot of the measured coverage of the surroundings n_s(crit) at invasion vs temperature. The error bars indicate that each invasion point may be in error by a maximum of ±1 dose of gold. Application of Eq. (7) (---), shows the expected dependence of n_s(crit) on temperature, and a greater dependence on a, the decrease in binding energy, than on n_p(crit).

stable nucleus is formed on the plane. The energy of binding to the nucleus will be higher than that to the plane, and rapid completion of a gold monolayer on the plane will ensue. Thus at the invasion point n_s and n_p will have critical values n_s(crit) and n_p(crit), respectively, and from Eq. (5), n_s(crit) can be expressed as

$$n_s(\text{crit}) = \frac{kT}{a} \ln \left[\frac{n_p(\text{crit})}{n_s(\text{crit})} \right] + \frac{[H_s(0) - H_p]}{a}. \tag{7}$$

Over the relevant range of n_s the logarithmic term will change only slightly, so that n_s(crit) should vary approximately linearly with temperature, and Fig. 6 shows this to be approximately true.

The value of a is not known, but a decrease in the binding energy of 1 eV during formation of a monolayer has been observed for silver (*15*) and lead (*16*), and we therefore assume that a = 1 eV. $H_s(0)$ for gold is 3.3 eV (*17*), and H_p = 2.2 eV (*4*). If we assume that the smallest stable nucleus is 2 atoms, on a 110 plane of 24 nm diameter, n_p(crit) = $4.42 * 10^{14}$ atoms/sq.m. Equation 5 can then be solved iteratively, n_s(crit), converging to within 1% in 3 iterations. The result is presented in figure 6 for n_p(crit) corresponding to 2, 3 and 10 atoms on the plane.

In an SEM study of silver nucleation on a macroscopic $W(110)$ surface in UHV, Spiller *et al.* (*18*) presented evidence for critical nuclei of size ranging from 2 to 46 atoms, but as they point out, on such surfaces steps will be important in nucleation. Thus although such steps are not present in the probed area, the assumption that just 2 atoms on the plane are required to form the required nucleus is likely to be an underestimate. However, as illustrated in Fig. 6, n_s(crit) is not strongly dependent on the chosen value of n_p(crit). The predicted values

of n_s(crit) are more strongly dependent on the parameter a (Fig. 6), and on the heats of binding, none of which are known with sufficient accuracy to throw further light on the nucleation mechanism. Despite the experimental uncertainties, we believe that the model does account satisfactorily for the observed behaviour.

Following invasion, Φ cannot be derived from FN data because β may also have changed. However, Bauer *et al.* (*19*), have shown that a complete monolayer of gold forms a 1 × 1 structure on *W*(110) resulting in an increase in Φ(110) which depends on the spreading temperature, ranging from 0.12 eV at 300 K to 0.20 eV at 900 K. We estimate the increase in Φ(110) for spreading at 750 K to be 0.150 eV; thus Φ(110) will be 5.40 eV, and from Eq. (1), β increases to 1.58 following invasion. Thus it seems that the entire decrease in V_p on invasion, Fig. 3, can be attributed to an increase in β, while Φ(110), coincidentally, remains unchanged despite acquiring a monolayer of gold.

Region 4. With increasing gold cover ΔV_p eventually becomes constant. Bauer et al. (*19*), using LEED, have shown that when the gold coverage exceeds 3 monolayers a strained Au(111) structure forms and $\Delta\Phi$(110) becomes approximately constant at 0.20 eV. If we assume this to be true in the present case then Φ(110) becomes 5.45 eV, and β decreases to 1.43, Fig. 3, which implies the restoration of a relatively smooth surface. At this stage Bauer *et al.* find a tendency to growth of 3-dimensional crystallites which, in the present case, should lead to an increase in roughness and a reduction in the emitting area A. The absence of nucleating steps on our (110) surfaces could account for the lack of any evidence for crystallite formation, but the reason for the observed increase in A is not clear. Presumably it reflects the development of the band structure of gold.

4.2. *Silver*

Field ion microscopy has shown that, unlike gold, adsorbed silver does not induce any rearrangement of the (110) environs (*13*), but does produce a considerable decrease in the work function of the plane (*20*). We have therefore examined silver invasion of the 110 plane by surface diffusion. The metal was vapor deposited from a Specpure source of similar construction to that used for gold. Particular attention had to be given to purging the source of residual oxygen as noted previously (*17*).

Figure 7 shows typical behavior of ΔV_t and ΔV_p with increasing silver concentration. The initial rise in ΔV_p is very small and exhibits no clearly measurable change with spreading temperature, but the increase in both Φ(110) and A with an accompanying decrease in β is similar to that seen with gold, and we propose that these also result from the widening of the 110 plane. Invasion is marked by a large decrease in ΔV_p to a value which remains constant with increasing silver coverage until at an adatom density of 3×10^{19} m^2 there is a further sharp drop to a final concentration-independent value. This behavior is quite unlike that of gold but is closely similar to invasion of W(110) by lead and copper, (*6*, *10*) and of Group 1b metal diffusion onto low-index planes of rhenium (*7*) and iridium, (*21*).

Monolayer silver on W(110) forms an Ag(111) structure which is strained in the 100 direction to fit the periodicity of W(110), and reduces Φ(110) by 0.60 eV (*19*). If we assume this to be the structure formed in the present case, then Φ(110) at the plateau becomes 4.65 ± 0.03 eV, and β is seen to have changed very little.

The dramatic decrease in A at coverages exceeding 2 monolayers is difficult to explain. It could result from formation of small 3-dimensional crystallites which become the dominant electron emitters, but there is no corresponding increase in β. Bauer *et al.*

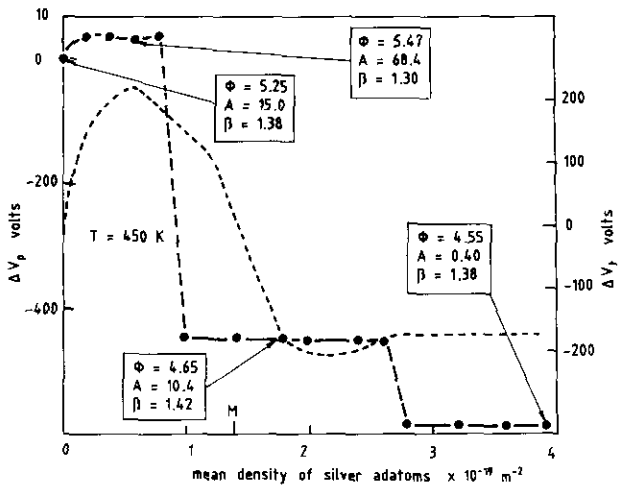

FIG. 7. Adsorption characteristic for silver on W(110), spread at 450 K, showing the work function ϕ (eV), the emitting area A (nm^2), and the field enhancement factor $\beta \times 10^{-4}$. ΔV_i(----).

observed small 3-D crystallites to grow on the second monolayer only at temperatures above 800 K (*19*), but Spiller *et al.* (*18*), detect crystallite growth before completion of the second layer and at temperatures below 600 K. Unlike gold, silver shows no dependence of plane invasion on spreading temperature.

5. Conclusions

1. Changes in work function (measured by Fowler–Nordheim analysis) which are observed at the center of W(110) when adsorbed gold or silver is allowed to surround the W(110) plane but not to invade it, result from a reduction in the local applied field due to expansion of the plane by adsorption of metal atoms in the terrace sites which surround the central plane.

2. At elevated temperatures gold-mediated diffusion of tungsten in the terrace regions reduces the emitting area leaving the work function and field strength at the plane centre unchanged. Adsorbed silver is known to be incapable of altering the tungsten substrate structure in the environs of (110), and in keeping with this there is no evidence of silver-mediated diffusion at elevated temperatures.

3. An abrupt reduction in V_p marks the invasion of the 110 plane by gold and the temperature-dependence of this step is consistent with a mechanism of invasion, nucleation, and rapid growth of a monolayer. By coincidence the work functions before and after invasion are almost identical, the invasion being marked only by change in the surface roughness. Invasion by silver produces a considerable change in work function but surprisingly, invasion shows no dependence on temperature.

4. Work functions cannot be measured beyond the invasion point, but if the values derived from the work of Bauer *et al.* are assumed, a consistent account of the observed changes can be presented for both gold and silver, in which the derived changes in β are physically plausible.

5. The 110 plane on an annealed tungsten field emitter tip remains a useful and uniquely well-defined environment for examining nucleation processes. It is step-free and defect-free and the techniques of field

ion microscopy can reveal the extent to which the substrate structure is altered. These microscopic techniques are best combined with parallel macroscopic studies, and the necessary contact between macro and micro investigations can be made through measurement of work function changes.

References

1. D. W. Bassett, *Proc. R. Soc. London Ser. A* **286,** 191, (1965).
2. C. D. Ehrlich and E. W. Plummer, *Phys. Rev. B* **18,** 3767, (1978).
3. A. Modinos and N. Nicolau, *Phys. Rev. B* **13,** 1536, (1976).
4. E. W. Plummer and T. N. Rhodin, *J. Chem. Phys.* **19,** 3479 (1968).
5. J. P. Jones and E. W. Roberts, *Thin Solid Films* **48,** 215 (1978).
6. J. P. Jones and E. W. Roberts, *Surf. Sci.* **62,** 415 (1977).
7. O. Z. AlRawi and J. P. Jones, *Surf. Sci.* **124,** 220 (1983).
8. A. van Oostrom, *Philips Res. Rep. Suppl.* **1,** 1966.
9. C. J. Todd and T. N. Rhodin, *Surf. Sci.* **36,** 353 (1973).
10. J. P. Jones and E. W. Roberts, *Surf. Sci.* **69,** 185 (1977).
11. R. D. Young and H. E. Clark, *Appl. Phys. Lett.* **9,** 265 (1966).
12. J. P. Jones, "Symposia on Surface Phenomena of Metals," Monograph No. 28, Soc. of Chem. Industry, London, (1967).
13. A. Cetronio and J. P. Jones, *Surf. Sci.* **40,** 227 (1973).
14. J. P. Jones and N. T. Jones, *Surf. Sci.* **35,** 83 (1976).
15. C. M. Lo and J. B. Hudson, *Thin Solid Films* **12,** 261 (1972).
16. J. M. Bermond, B. Felts, and M. Drechsler, *Surf. Sci.* **49,** 207 (1975).
17. A. Cetronio and J. P. Jones, *Thin Solid Films* **35,** 113 (1976).
18. G. D. T. Spiller, P. Akhter, and J. Venables, *Surf. Sci.* **131,** 517 (1983).
19. E. Bauer, H. Poppa, G. Todd, and P. R. Davies, *J. Appl. Phys.* **48,** 3773 (1977).
20. Z. Sidorski, T. Szelwicki, and Z. Dworechi, *Thin Solid Films* **61,** 203 (1979).
21. K. I. Hashim, Ph.D. Thesis, Univ. of Wales, 1987.